J|A|C|S ARTICLES

Published on Web 02/19/2009

Liquid Phase Production of Graphene by Exfoliation of Graphite in Surfactant/Water Solutions

Mustafa Lotya,[†] Yenny Hernandez,[†] Paul J. King,[†] Ronan J. Smith,[†] Valeria Nicolosi,[‡] Lisa S. Karlsson,[‡] Fiona M. Blighe,[†] Sukanta De,[†,§] Zhiming Wang,[†] I. T. McGovern,[†] Georg S. Duesberg,[§,||] and Jonathan N. Coleman*[,†,§]

School of Physics, Trinity College Dublin, Dublin 2, Ireland, Department of Materials, University of Oxford, Parks Road, Oxford OX1 3PH, United Kingdom, CRANN, Trinity College Dublin, Dublin 2, Ireland, and School of Chemistry, Trinity College Dublin, Dublin 2, Ireland

Received September 29, 2008; E-mail: colemaj@tcd.ie

Abstract: We have demonstrated a method to disperse and exfoliate graphite to give graphene suspended in water−surfactant solutions. Optical characterization of these suspensions allowed the partial optimization of the dispersion process. Transmission electron microscopy showed the dispersed phase to consist of small graphitic flakes. More than 40% of these flakes had <5 layers with ∼3% of flakes consisting of monolayers. Atomic resolution transmission electron microscopy shows the monolayers to be generally free of defects. The dispersed graphitic flakes are stabilized against reaggregation by Coulomb repulsion due to the adsorbed surfactant. We use DLVO and Hamaker theory to describe this stabilization. However, the larger flakes tend to sediment out over ∼6 weeks, leaving only small flakes dispersed. It is possible to form thin films by vacuum filtration of these dispersions. Raman and IR spectroscopic analysis of these films suggests the flakes to be largely free of defects and oxides, although X-ray photoelectron spectroscopy shows evidence of a small oxide population. Individual graphene flakes can be deposited onto mica by spray coating, allowing statistical analysis of flake size and thickness. Vacuum filtered films are reasonably conductive and are semitransparent. Further improvements may result in the development of cheap transparent conductors.

1. Introduction

The discovery of monolayer graphene in 2004[1] has led to the demonstration of a host of novel physical properties in this most exciting of nanomaterials.[2] Graphene is generally made by micromechanical cleavage, a process whereby monolayers are peeled from graphite crystals. However, this process has significant disadvantages in terms of yield and throughput. As such, there has been significant interest in the development of a large-scale production method for graphene. In the long term, for many research areas the growth of graphene monolayers[3−5] is by far the most desirable route. However, progress has been slow, and, in any case, this technique will be unsuitable for certain applications. Thus, in the medium term, the most promising route is the exfoliation of graphite in the liquid phase to give graphene-like materials. The most common technique has been the oxidation and subsequent exfoliation of graphite to give graphene oxide.[6−10] However, this technique suffers from one significant disadvantage; the oxidation process results in the formation of structural defects as evidenced by Raman spectroscopy.[6,9] These defects alter the electronic structure of graphene so much as to render it semiconducting.[11] These defects are virtually impossible to remove completely; even after annealing at 1100 °C, residual C═O and C−O bonds are observed by X-ray photoelectron spectroscopy.[10] Even relatively mild chemical treatments, involving soaking in oleum, result in non-negligible oxidation, which requires annealing at 800 °C to remove.[12]

[†] School of Physics, Trinity College Dublin.
[‡] University of Oxford.
[§] CRANN, Trinity College Dublin.
[||] School of Chemistry, Trinity College Dublin.

(1) Novoselov, K. S.; Geim, A. K.; Morozov, S. V.; Jiang, D.; Zhang, Y.; Dubonos, S. V.; Grigorieva, I. V.; Firsov, A. A. *Science* **2004**, *306*, 666–669.
(2) Geim, A. K.; Novoselov, K. S. *Nat. Mater.* **2007**, *6*, 183–191.
(3) Berger, C.; Song, Z. M.; Li, X. B.; Wu, X. S.; Brown, N.; Naud, C.; Mayo, D.; Li, T. B.; Hass, J.; Marchenkov, A. N.; Conrad, E. H.; First, P. N.; de Heer, W. A. *Science* **2006**, *312*, 1191–1196.
(4) Ohta, T.; El Gabaly, F.; Bostwick, A.; McChesney, J. L.; Emtsev, K. V.; Schmid, A. K.; Seyller, T.; Horn, K.; Rotenberg, E. *New J. Phys.* **2008**, 10.
(5) Kim, K. S.; Zhao, Y.; Jang, H.; Lee, S. Y.; Kim, J. M.; Kim, K. S.; Ahn, J.-H.; Kim, P.; Choi, J.-Y.; Hong, B. H. *Nature* **2009**, *457*, 706−710.
(6) Eda, G.; Fanchini, G.; Chhowalla, M. *Nat. Nanotechnol.* **2008**, *3*, 270–274.
(7) Li, D.; Muller, M. B.; Gilje, S.; Kaner, R. B.; Wallace, G. G. *Nat. Nanotechnol.* **2008**, *3*, 101–105.
(8) Niyogi, S.; Bekyarova, E.; Itkis, M. E.; McWilliams, J. L.; Hamon, M. A.; Haddon, R. C. *J. Am. Chem. Soc.* **2006**, *128*, 7720–7721.
(9) Stankovich, S.; Dikin, D. A.; Piner, R. D.; Kohlhaas, K. A.; Kleinhammes, A.; Jia, Y.; Wu, Y.; Nguyen, S. T.; Ruoff, R. S. *Carbon* **2007**, *45*, 1558–1565.
(10) Becerril, H. A.; Mao, J.; Liu, Z.; Stoltenberg, R. M.; Bao, Z.; Chen, Y. *ACS Nano* **2008**, *2*, 463–470.
(11) Jung, I.; Pelton, M.; Piner, R.; Dikin, D. A.; Stankovich, S.; Watcharotone, S.; Hausner, M.; Ruoff, R. S. *Nano Lett.* **2007**, *7*, 3569–3575.

Recently, a significant breakthrough was made when two independent groups showed that graphite could be exfoliated in certain solvents to give defect-free monolayer graphene.[13,14] This phenomenon relies on using particular solvents, such as *N*-methyl-pyrrolidone, whose surface energy is so well matched to that of graphene that exfoliation occurs freely.[14] However, this process is not without its drawbacks. These solvents are expensive and require special care when handling. In addition, they tend to have high boiling points, making it difficult to deposit individual monolayers on surfaces. Unfortunately, the most useful solvent of all, water, has a surface energy that is much too high to work on its own as an exfoliant for graphene.

With these factors in mind, it is easy to see what is needed. We require an alternative, liquid phase process that results in the exfoliation of graphite to give graphene at reasonably high yield. The method should be non-oxidative and should not require high temperature processes or chemical post treatments. In addition, it should be compatible with safe, user-friendly, low boiling-point solvents, preferably water.

In this Article, we demonstrate such a method. We disperse graphite in surfactant−water solutions in a manner similar to surfactant aided carbon nanotube dispersion.[15−20] By transmission electron microscopy (TEM) analysis, we demonstrate significant levels of exfoliation including the observation of a number of graphene monolayers. Atomic resolution TEM shows the monolayers to be well graphitized and largely defect free. Raman, IR, and X-ray photoelectron spectroscopies also show the graphite/graphene to be relatively defect free and only very slightly oxidized. These dispersions can be vacuum filtered to make thin conductive films and deposited onto surfaces as individual flakes.

2. Results and Discussion

2.1. Optimization of Dispersion Conditions. The absorption coefficient, α, which is related to the absorbance, *A*, through the Lambert−Beer law ($A = \alpha Cl$, where *C* is the concentration and *l* is the path length), is an important parameter in characterizing any dispersion. To accurately determine α, we prepared a dispersion (~400 mL) with initial graphite concentration, $C_{G,i} = 0.1$ mg/mL, and surfactant (sodium dodecylbenzene sulfonate, SDBS) concentration, $C_{SDBS} = 0.5$ mg/mL. This was then centrifuged and decanted, and the absorption spectrum was measured (inset of Figure 1). As expected for a quasi two-dimensional material, this spectrum is flat and featureless[21] everywhere except below 280 nm where we observe a strong absorption band, which scaled linearly with SDBS concentration but was independent of the graphite concentration; we attribute this band to the SDBS. A precisely measured volume of the dispersion was filtered under high vacuum onto an alumina membrane of known mass. The resulting compact but relatively thick film (~5 μm) was washed with 1 L of water and dried overnight in a vacuum oven at room temperature. The mass of material in the filtered volume of stock dispersion was then determined using a microbalance. From thermogravimetric (TGA) analysis (not shown) of the dried film, we found that 64 ± 5% of the film was graphitic; the remainder was attributed to residual surfactant. We are not surprised to find so much residual surfactant in these films. Their considerable thickness (~5 μm) makes it very difficult to wash away the surfactant during film formation. Knowledge of the mass of graphite in the film allowed us to determine the final concentration of the stock dispersion. A sample of the stock dispersion was then serially diluted with 0.5 mg/mL SDBS solution, allowing the measurement of the absorbance per unit length (*A*/*l*) versus concentration of graphite (after centrifugation, C_G), as shown in Figure 1. A straight line fit through these points gives the absorption coefficient at 660 nm of $\alpha = 1390$ mL mg^{-1} m^{-1} in reasonable agreement with the value measured for graphite/graphene in various solvents.[14] The non-zero intercept in Figure 1 is attributable to the *A*/*l* of residual SDBS in the dispersion (intercept of $A/l = 0.72$ m^{-1} compares with residual absorbance of $A/l \approx 0.5$ m^{-1} for SDBS at $C_{SDBS} = 0.5$ mg/mL).

Using α for our dispersions, it is possible to determine C_G for all subsequent samples. Thus, the fraction of graphite material remaining for any sample after centrifugation (CF) can be calculated from the ratio of dispersed graphite after CF to that before CF: $C_G/C_{G,i}$. Using this fraction-remaining as a gauge, the concentrations $C_{G,i}$ and C_{SDBS} could be optimized. Holding

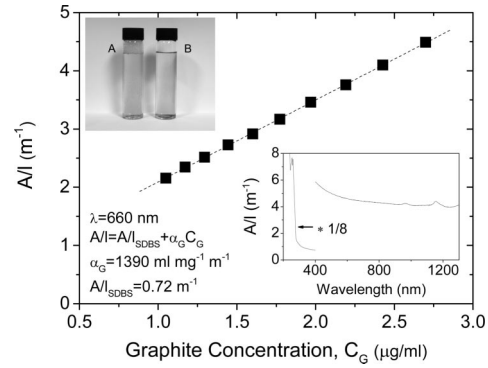

Figure 1. Absorbance per unit length ($\lambda = 660$ nm) as a function of graphite concentration (after centrifugation) for an SDBS concentration, $C_{SDBS} = 0.5$ mg/mL. Graphite concentration before centrifugation was $C_{G,i} = 0.1$ mg/mL. NB, the curve does not go through the origin due to the presence of a residual SDBS absorbance. (Intercept of $A/l = 0.72$ m^{-1} compares with residual absorbance of $A/l \approx 0.5$ m^{-1} for SDBS at $C_{SDBS} = 0.5$ mg/mL.) Bottom inset: Absorption spectrum for a sample with $C_{SDBS} = 0.5$ mg/mL and $C_G = 0.0027$ mg/mL. The portion below 400 nm is dominated by the surfactant absorption and has been scaled by a factor of 1/8 for clarity. The portion above 400 nm is dominated by graphene/graphite with some residual SDBS absorption. Top inset: Surfactant-stabilized graphite dispersions (A) before and (B) immediately after centrifugation. Note that the dispersions are almost transparent due to the low concentration of graphite.

(12) Li, X.; Zhang, G.; Bai, X.; Sun, X.; Wang, X.; Wang, E.; Dai, H. *Nat. Nanotechnol.* **2008**, *3*, 538–542.
(13) Blake, P.; Brimicombe, P. D.; Nair, R. R.; Booth, T. J.; Jiang, D.; Schedin, F.; Ponomarenko, L. A.; Morozov, S. V.; Gleeson, H. F.; Hill, E. W.; Geim, A. K.; Novoselov, K. S. *Nano Lett.* **2008**, *8*, 1704–1708.
(14) Hernandez, Y.; et al. *Nat. Nanotechnol.* **2008**, *3*, 563–568.
(15) Moore, V. C.; Strano, M. S.; Haroz, E. H.; Hauge, R. H.; Smalley, R. E.; Schmidt, J.; Talmon, Y. *Nano Lett.* **2003**, *3*, 1379–1382.
(16) O'Connell, M. J.; Bachilo, S. M.; Huffman, C. B.; Moore, V. C.; Strano, M. S.; Haroz, E. H.; Rialon, K. L.; Boul, P. J.; Noon, W. H.; Kittrell, C.; Ma, J. P.; Hauge, R. H.; Weisman, R. B.; Smalley, R. E. *Science* **2002**, *297*, 593–596.
(17) O'Connell, M. J.; Boul, P.; Ericson, L. M.; Huffman, C.; Wang, Y. H.; Haroz, E.; Kuper, C.; Tour, J.; Ausman, K. D.; Smalley, R. E. *Chem. Phys. Lett.* **2001**, *342*, 265–271.
(18) Strano, M. S.; Moore, V. C.; Miller, M. K.; Allen, M. J.; Haroz, E. H.; Kittrell, C.; Hauge, R. H.; Smalley, R. E. *J. Nanosci. Nanotechnol.* **2003**, *3*, 81–86.
(19) Bergin, S. D.; Nicolosi, V.; Cathcart, H.; Lotya, M.; Rickard, D.; Sun, Z. Y.; Blau, W. J.; Coleman, J. N. *J. Phys. Chem. C* **2008**, *112*, 972–977.
(20) Sun, Z.; Nicolosi, V.; Rickard, D.; Bergin, S. D.; Aherne, D.; Coleman, J. N. *J. Phys. Chem. C* **2008**, *112*, 10692–10699.
(21) Abergel, D. S. L.; Fal'ko, V. I. *Phys. Rev. B* **2007**, 75.

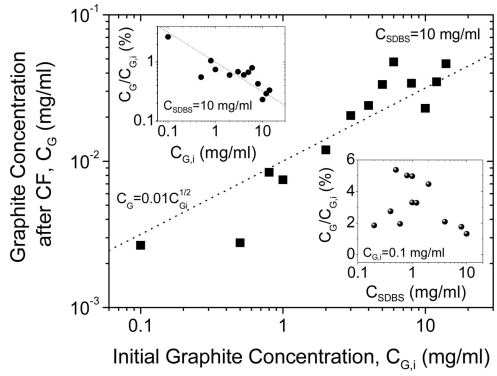

Figure 2. Graphite concentration after centrifugation (CF) as a function of starting graphite concentration (C_{SDBS} = 10 mg/mL). Upper inset: The same data represented as the fraction of graphite remaining after CF. Lower inset: Fraction of graphite after centrifugation as a function of SDBS concentration ($C_{G,i}$ = 0.1 mg/mL).

C_{SDBS} constant at a relatively high value of 10 mg/mL, C_G was measured as a function of $C_{G,i}$ (Figure 2). Interestingly, we observe an empirical relationship of the form: $C_G = 0.01\sqrt{C_{G,i}}$. The highest concentration achieved after CF was C_G = 0.05 mg/mL for $C_{G,i}$ = 14 mg/mL. We have observed concentrations in the range 0.002 mg/mL < C_G < 0.05 mg/mL. We note that this is very similar to the range of concentrations generally achieved for surfactant-stabilized nanotube dispersions.[22] The largest fraction remaining was ~3 wt % at $C_{G,i}$ = 0.1 mg/mL (top inset, Figure 2). This graphite concentration was then fixed and C_{SDBS} varied. Measurement of the fraction remaining showed a broad peak (lower inset, Figure 2), similar to those observed for nanotube−surfactant dispersions.[19] The graphitic content was maximized for C_{SDBS} between 0.5 and 1 mg/mL, concentrations very close to the critical micelle concentration (CMC), which is ~0.7 mg/mL for SDBS.[23] The falloff in dispersed graphite below $C_{SDBS} \approx$ 0.5 mg/mL is reminiscent of the destabilization of nanotube dispersions as the surfactant concentration is reduced below the CMC.[19,24] With this in mind, we can hypothesize that the minimum surfactant concentration required for successful dispersion of graphite is the critical micelle concentration. If this is the case, the surfactant concentration could possibly be reduced by using alternative surfactants with lower CMC. In this work, to keep the concentration of surfactant to a minimum, all subsequent experiments were performed on standard dispersions with surfactant concentration close to the CMC: C_{SDBS} = 0.5 mg/mL (also $C_{G,i}$ = 0.1 mg/mL). (NB, the fraction remaining in the experiment described in Figure 1, was much smaller than would be expected from the data shown in Figure 2. This is due to the fact that in the former experiment a much larger volume was used resulting in less efficient sonication.)

2.2. Evidence of Exfoliation. To further characterize the exact form of nanocarbons in the dispersions, we conducted a detailed TEM analysis of our standard dispersion. TEM samples were prepared by pipetting a few milliliters of this dispersion onto holey carbon mesh grids (400 mesh). TEM analysis revealed a large quantity of flakes of different types as shown in Figure 3. A small quantity of monolayer graphene flakes was observed (Figure 3A). A larger proportion of flakes were few-layer graphene, including some bilayers and trilayers as shown in Figure 3B and C. In addition, a number of rather disordered flakes with many layers, similar to the one in Figure 3D, were observed. The disorder suggests that these flakes formed by reaggregation of smaller flakes. Finally, a very small number (2) of very large flakes were observed (Figure 3E). It can be shown that these are graphite by the observation of thin multilayers protruding from their edges (Figure 3E, inset). Note that while these large flakes are rare when counted by number, they will contribute disproportionally by mass. It is possible to estimate the number of layers per flake for all but the largest flakes. These data are illustrated in the histogram for the standard dispersion in Figure 4A (the very large flakes are ignored in this histogram). These statistics show a reasonable population of few-layer graphene. For example, ~43% of flakes had <5 layers. More importantly, ~3% of the flakes were monolayer graphene. While this value is considerably smaller than that observed for graphene/solvent dispersions,[14] working in aqueous systems brings its own advantages. In general, the majority of these few-layer flakes had lateral dimensions of ~1 μm. Thicker

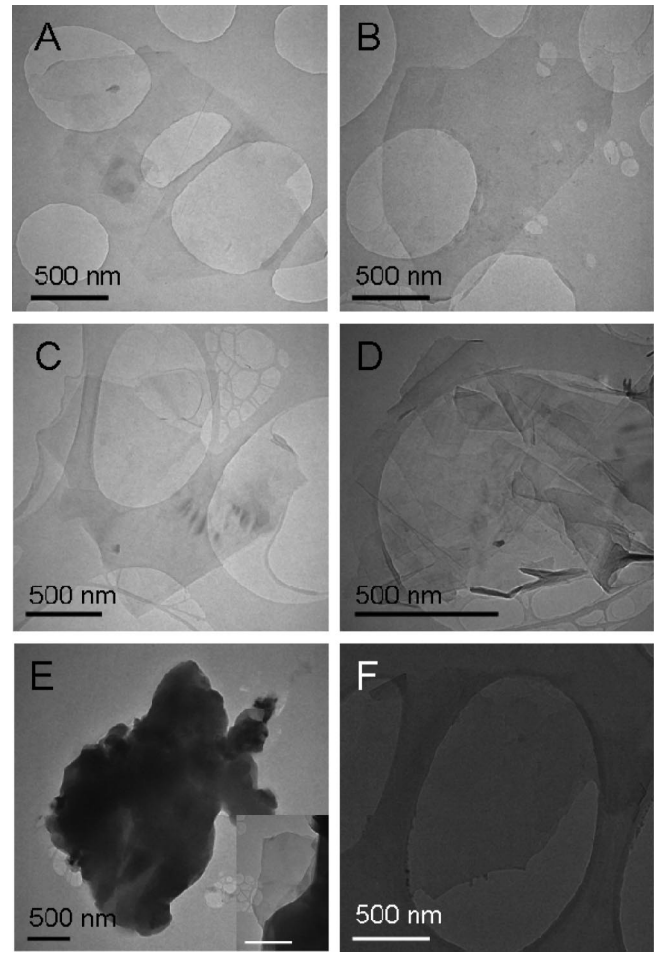

Figure 3. Selected TEM images of flakes prepared by surfactant processing. (A) A monolayer (albeit with a small piece of square debris close to its left-hand edge). (B) A bilayer. (C) A trilayer. (D) A disordered multilayer. (E) A very large flake. Inset: A closeup of an edge of a very large flake showing a small multilayer graphene flake protruding. (F) A monolayer from a sample prepared by sediment recycling.

(22) Bergin, S. D.; Nicolosi, V.; Streich, P. V.; Giordani, S.; Sun, Z.; Windle, A. H.; Ryan, P.; Peter, N.; Niraj, P.; Wang, Z.-T. T.; Carpenter, L.; Blau, W. J.; Boland, J. J.; Hamilton J. P.; Coleman, J. N. *Adv. Mater.* **2008**, *20*, 1876−1881.
(23) Lockwood, N. A.; de Pablo, J. J.; Abbott, N. L. *Langmuir* **2005**, *21*, 6805.
(24) McDonald, T. J.; Engtrakul, C.; Jones, M.; Rumbles, G.; Heben, M. J. *J. Phys. Chem. B* **2006**, *110*, 25339–25346.

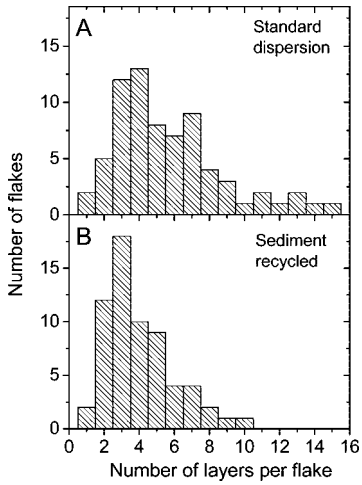

Figure 4. Histogram of number of layers per flake for dispersions from original sieved graphite and from recycled sediment. This histogram does not include the two very large flakes of the type shown in Figure 3E.

flakes, with more than a few graphene layers per flake, were larger, ranging up to 3 μm in diameter.

The sediment remaining after centrifugation can be recycled to improve the overall yield of graphene exfoliation. The sediment was recovered, and fresh (0.5 mg/mL) SDBS solution was added. This sediment dispersion was then processed in the same manner as the original dispersion, and TEM analysis was carried out. In this case, we also observed the presence of isolated monolayer graphene in about 3% of cases (Figure 3F). In addition, the flake thickness distribution shifted toward thinner flakes with large quantities of bilayers and trilayers; 67% of flakes observed had <5 layers (Figure 4B). Notably, there were no large flakes with greater than 10 layers observed, indicating that the reprocessing of recycled sediment gives better exfoliation than processing of the original sieved graphite. We suggest that the second sonication breaks up the already partially exfoliated chunks of graphite into even smaller pieces from which exfoliation occurs more easily.

The ability to easily deposit graphene flakes on a TEM grid allows their detailed characterization using high-resolution TEM (HRTEM). We can use this to confirm the presence of graphene monolayers in these surfactant-stabilized dispersions. Shown in Figure 5A is a HRTEM image of a graphene monolayer similar to that shown in Figure 3A. Significant nonuniformities can be seen, suggesting the presence of residual surfactant. The inset depicts a fast Fourier transform (FFT) of this image. This is equivalent to an electron diffraction pattern. The {1100} spots can clearly be seen. However, the {2110} spots are too faint to see. This intensity difference is the fingerprint of monolayer graphene.[14,25] In contrast, a HRTEM image of a graphene multilayer is shown in Figure 5B. This identification is based on the observation of more than one monolayer at the edge of the flake. In this case, the diffraction pattern (inset) clearly shows the {1100} and {2110} spots. Furthermore, the {2110} spots are clearly more intense, confirming that this is a multilayer.[14]

We can employ aberration correctors to further improve image quality. Shown in Figure 5C is an aberration corrected HRTEM image of a graphene monolayer as identified via the FFT (inset). This image reveals nonuniformity in the phase contrast transfer, most likely due to the presence of residual surfactant, although the presence of other kinds of structural anomalies such as ripples cannot be discounted. A careful focal series exit-wave function restoration is currently in progress to determine their nature. A fast Fourier transform of the area indicated by the white square is shown in the inset, revealing diffractions typical of single layer graphene.[14] A filtered image of part of the region enclosed by the white square in Figure 5C is shown in Figure 5D (Fourier mask filtering, twin-oval patter, edge smoothed by 5 pixels). This filtered image is of atomic resolution and clearly illustrates the hexagonal nature of the graphene. Intensity analysis (Figure 5E) along the left dashed line shows a hexagon width of 2.4 Å, close to the expected value of 2.5 Å. In addition, analysis of the intensity profile along the right dashed line (Figure 5F) gives the C−C bond length of 1.44 Å, close to the expected value of 1.42 Å. Most importantly, all imaged areas appeared to be largely free of structural defects, showing that this exfoliation technique is nondestructive.

2.3. Dispersion Stability. The zeta potential is a useful parameter we can use to characterize our dispersions. SDBS is an ionic surfactant that is expected to adsorb onto the graphene flakes and impart an effective charge. We expect that the dispersions will be stabilized by electrostatic repulsion between surfactant-coated graphene flakes. This mechanism has allowed the successful dispersion of carbon nanotubes in a range of surfactants.[19,22,26,27] The zeta potential is the potential at the interface between the adsorbed surfactant molecular ions and the diffuse region of mobile counterions. As such, it is a measure of the electrostatic repulsion between surfactant-coated flakes. We apply the Smoluchowski expression[28] for plate-like particles in our calculations. This is identical to the Smoluchowski approximation[29] for spherical particles, which was previously used in relation to carbon nanotube dispersions in SDBS.[20,26] The natural pH of our dispersions was 7.4, which matches a literature value for SDBS-stabilized carbon nanotube dispersions.[26]

We observed a zeta potential distribution for a fresh graphite/graphene dispersion centered at −44 mV (Figure 6A). The shoulder at −76 mV is probably due to free surfactant, as it matches well to the position of the zeta spectrum of a 0.5 mg/mL SDBS solution at −71 mV (Figure 6A). For fresh graphite/graphene, the peak zeta potential of −44 mV is well beyond the accepted value for colloidal stability of −25 mV, indicating that reaggregation should be minimized. For comparison, the zeta spectrum of a 6 week old graphene/graphite dispersion is also shown. This spectrum is peaked at −78 mV with a shoulder at −103 mV. We suggest the peak is due to unbound surfactant, while the shoulder is due to surfactant-coated graphite/graphene flakes. That the zeta potential has shifted to more negative values over 6 weeks strongly suggests that the electrophoretic mobility, μ, has increased in magnitude. One explanation for this could be a reduction in mean flake size, which should increase the electrophoretic mobility and hence the zeta potential in nonspherical samples (this is due to shape-dependent corrections to Stokes law for nonspherical particles[30]). The origin of such a size reduction will be discussed below.

(25) Meyer, J. C.; Geim, A. K.; Katsnelson, M. I.; Novoselov, K. S.; Booth, T. J.; Roth, S. *Nature* **2007**, *446*, 60–63.
(26) White, B.; Banerjee, S.; O'Brien, S.; Turro, N. J.; Herman, I. P. *J. Phys. Chem. C* **2007**, *111*, 13684–13690.
(27) Matarredona, O.; Rhoads, H.; Li, Z. R.; Harwell, J. H.; Balzano, L.; Resasco, D. E. *J. Phys. Chem. B* **2003**, *107*, 13357–13367.
(28) Ohshima, H. *Theory of Colloid and Interfacial Electric Phenomena*; Elsevier: New York, 2006.
(29) Michov, B. M. *Electrophoresis* **1988**, *9*, 199–200.
(30) Atkins, P. W. *Physical Chemistry*, 4th ed.; Oxford University Press: Oxford, 1990.

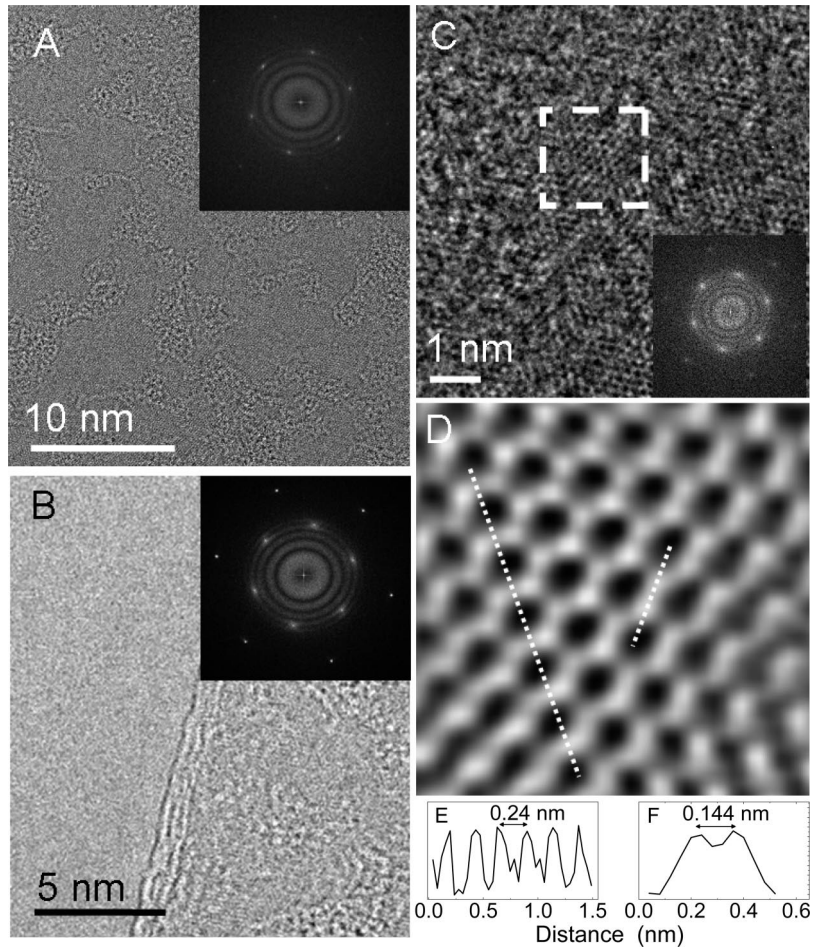

Figure 5. High-resolution TEM images of surfactant exfoliated graphene flakes. (A) A HRTEM image of a section of a graphene monolayer. Inset: Fast Fourier transform (equivalent to an electron diffraction pattern) of the image. (B) HRTEM image of a section of a trilayer. Inset: Fast Fourier transform of the image. (C) HRTEM image of part of a graphene monolayer. Inset: Fast Fourier transform of the region enclosed by the white square. The scale bar is 1 nm. (D) A filtered image of part of the region in the white square. (E) Intensity analysis along the left white dashed line shows a hexagon width of 2.4 Å. (F) Intensity analysis along the right white dashed line shows a C−C bond length of 1.44 Å.

The pH of the fresh dispersion was varied by addition of HCl and NaOH with the results given in Figure 6A (inset). There is a trend toward more negative zeta potential values as the pH is raised; this suggests that interparticle repulsions are increased as more negative OH^- charges are added to the flakes. For acidic dispersions at lower pH values, a less negative zeta potential is found, consistent with charge neutralization and destabilization of the system. The zeta potential versus pH trend is in line with trends reported for graphene oxide and reduced graphene oxide colloids.[7] By lowering the pH, the zeta potential approaches the limit of stability in our system, but it does not pass through the isoelectric point. This may be due to very high surface coverage of graphene flakes by SDBS ionic molecules and perhaps also due to a buffer-like action by the free surfactant in the dispersion.

After centrifugation, these surfactant-stabilized graphene dispersions are relatively stable. Only moderate sedimentation and reaggregation has been observed for any of the samples presented in Figure 2 over a period of months. This includes the dispersions with lower surfactant concentrations (down to $C_{SDBS} = 0.1$ mg/mL). To quantitatively determine the temporal stability of these dispersions, we conducted sedimentation experiments on a centrifuged, decanted dispersion ($C_G = 0.006$ mg/mL, $C_{SDBS} = 0.5$ mg/mL). The optical absorbance of the sample at 650 nm was monitored as a function of time as shown in Figure 6B. The measured absorbance fell steadily, indicating sedimentation of approximately two-thirds of the material over a considerable period of time. A biexponential function could be fitted to the profile, indicating one stable and two sedimenting components.[31] The fit parameters indicate that 35 wt % of the sample is stable over the time frame of 35 days. We attribute this component to small flakes. Of the rest, 19 wt % of the flakes fall out rapidly, with a time constant of 21.5 h, while a further 46 wt % fall out over longer time scales (time constant ~208 h). As the time constant is related to the dimensions of the sedimenting object,[31] we can attribute the slowly and rapidly sedimenting objects to medium- and large-sized flakes, respectively. We suggest that the large flakes are fragments of graphite that inadvertently remained in the dispersion after decantation and that we can associate with the type of flake observed in Figure 3E. We identify the medium-sized flakes as those objects represented at the right side of the histogram in Figure 4A. TEM analysis of the 6 week old sample used for zeta measurements showed only small flakes remain; these were typically few-layer graphene flakes less than 500 nm in diameter. This confirms both that medium to large flakes are unstable and sediment out

(31) Nicolosi, V.; Vrbanic, D.; Mrzel, A.; McCauley, J.; O'Flaherty, S.; McGuinness, C.; Compagnini, G.; Mihailovic, D.; Blau, W. J.; Coleman, J. N. *J. Phys. Chem. B* **2005**, *109*, 7124–7133.

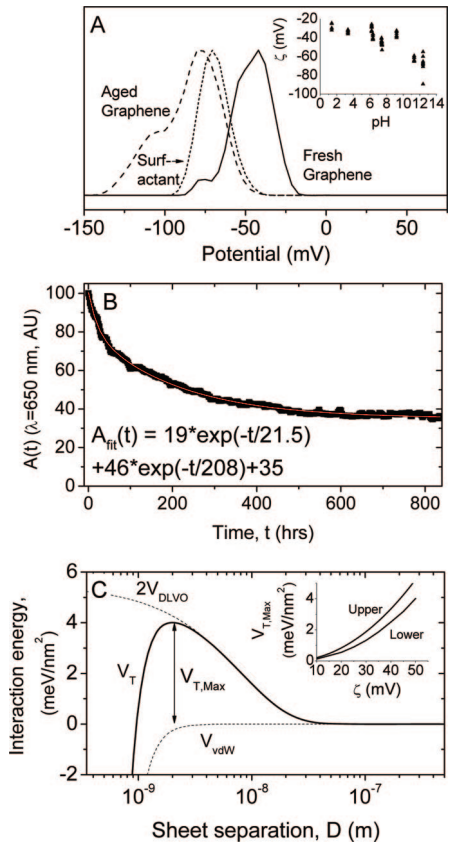

Figure 6. (A) Zeta spectra for a fresh graphene−SDBS dispersion (C_{SDBS} = 0.5 mg/mL, C_G = 0.006 mg/mL), an SDBS dispersion (C_{SDBS} = 0.5 mg/mL), and an aged (6 week old) graphene−SDBS dispersion (C_{SDBS} = 0.5 mg/mL, C_G = 0.0002 mg/mL). NB, the aged sample had a reduced C_G due to sedimentation over the course of 6 weeks. Inset: Zeta potential as a function of pH for SDBS−graphene dispersions (C_{SDBS} = 0.5 mg/mL, C_G = 0.005 mg/mL). The natural pH of the as-prepared graphene−SDBS dispersion was 7.4, and the pH was varied by addition of HCl or NaOH solution. (B) Absorbance (λ =650 nm) as a function of time for a C_G = 0.006 mg/mL, C_{SDBS} = 0.5 mg/mL sample. The curve has been fitted to a double exponential decay with the fit constants shown in the annotation. (C) Plot of the total interaction potential energy per unit area for two charged, parallel sheets separated by a distance D. The DLVO and vdW components are also shown for comparison. This graph was calculated using eq 1 and taking $\varepsilon_r = 80$, $\kappa^{-1} = 8.1$ nm, $\zeta = 50$ mV, and $\rho^2 C = 6.69 \times 10^{-40}$ J m^2. Inset: Graph of upper and lower limits of $V_{T,Max}$, as a function of zeta potential.

over 6 weeks (~1000 h) and that the increase in $|\zeta|$ is due to an increase in $|\mu|$ caused by the reduction in flake size over time.

2.4. Stabilization Mechanism. Having confirmed that the dispersed sheets are charged, we can consider the mechanism of stabilization of the surfactant-coated graphene. Stabilization of charged colloids is usually described via DLVO theory.[32] In this framework, surfactant-stabilized colloids are considered in terms of a layer of bound molecular ions (tail groups) and a diffuse cloud of counterions, the so-called double-layer. In this scenario, when viewed from afar, the colloid appears charged. As described above, the zeta potential is a measure of the effective charge. DLVO theory considers the balance of these repulsive interactions and attractive van der Waals (vdW) interactions between adjacent colloids. The attractive van der Waals potential energy between two parallel, two-dimensional sheets can be approximated as the sum of pairwise interatom attraction energies. This can be calculated (see Supporting Information) in a manner similar to the method pioneered by Hamaker[32,33] to be $V_{vdW} = -A\pi\rho^2 C/2D^4$, where A is the sheet area, ρ is the number of atoms per unit area in the sheets, D is the sheet separation, and C is the constant relating the interatomic van der Waals energy to the interatomic separation, $V = -C/r^6$. The repulsive DLVO potential energy for two charged surfaces is given by[32] $V_{DLVO} \approx 2A\varepsilon_r\varepsilon_0\kappa\zeta^2 e^{-\kappa D}$, where ζ is the zeta potential and κ^{-1} is the Debye screening length (a measure of the double layer thickness): $\kappa^{-1} = (\varepsilon_r\varepsilon_0 kT/2e^2 n_0)^{1/2}$ (n_0 is the number of surfactant molecules per unit volume of solution). We note that this expression only strictly holds for $|\zeta| < 25$ mV. However, we use it here to illustrate the mechanism, realizing that any numbers generated will be approximate. We find the interaction energy for two charged two-dimensional sheets by multiplying V_{DLVO} by 2 (to account for the fact that both sides of the sheets are charged). The overall potential energy of two parallel, two-dimensional sheets can thus be written as:

$$V_T \approx 4A\varepsilon_r\varepsilon_0\kappa\zeta^2 e^{-\kappa D} - A\pi\rho^2 C/2D^4 \quad (1)$$

In our dispersions, typically $C_{SDBS} = 0.5$ mg/mL. This means $n_0 = 8.6 \times 10^{23}$ m^{-3}, giving $\kappa^{-1} = 8.1$ nm. At neutral pH, we have measured $\zeta \approx -50$ mV. By considering the surface energy of graphite, which is approximately[14] 70 mJ/m^2, we can calculate $\rho^2 C = 6.69 \times 10^{-40}$ J m^2 (Supporting Information). Using these numbers, we can calculate V_T/A for a typical surfactant-stabilized graphene dispersion as a function of sheet separation, D. This is shown in Figure 6C. In addition, plots of the DLVO and vdW components, $2V_{DLVO}$ and V_{vdW}, are also included. It is clear from this graph that nearby graphene sheets feel a potential barrier, $V_{T,Max}$, which opposes aggregation. It is the presence of this barrier that results in the stabilization of surfactant-coated graphene sheets.

However, we note that we have most likely overestimated V_{vdW}, as our crude analysis ignores screening of the vdW interaction due to the solvent. Such screening can dramatically reduce the strength of the vdW attraction.[32] This means that the value of $V_{T,Max}$ presented in Figure 6C is a lower bound. We can estimate the upper bound by considering the extreme case, where screening has rendered the attractive interaction to be negligible. In this circumstance, the barrier is the value of V_{DLVO} for the minimum intersheet separation, $D \approx 0.35$ nm. A glance at Figure 6C shows that these bounds are actually close together. We have calculated the upper and lower bounds for $V_{T,Max}$ as a function of zeta potential as shown in the inset. Typical values for $V_{T,Max}$ lie in the range 2−4 meV/nm^2 for zeta between 40 and 60 mV. These values are quite large for the flakes observed in our dispersions: ~3000 eV for a 1 μm × 1 μm flake. Note that the model described above is approximate in a number of different ways (see above and Supporting Information). Nevertheless, we believe that this simple model captures the physics of the stabilization mechanism.

2.5. Graphene Films: Characterization and Potential Applications. To examine the film quality and potential uses of aqueous graphene dispersions, films were cast onto porous membranes by vacuum filtration. These films were washed with between 20 and 100 mL of Millipore water and dried overnight in a room temperature vacuum oven at ~1 × 10^{-3} mbar to remove the water. The film thickness, t, could be estimated from the known deposited mass per unit area, M/A, using $t = (M/$

(32) Israelachvili, J. *Intermolecular and Surface Forces*; Academic Press: New York, 1991.

(33) Hamaker, H. C. *Physica* **1937**, *4*, 1058–1072.

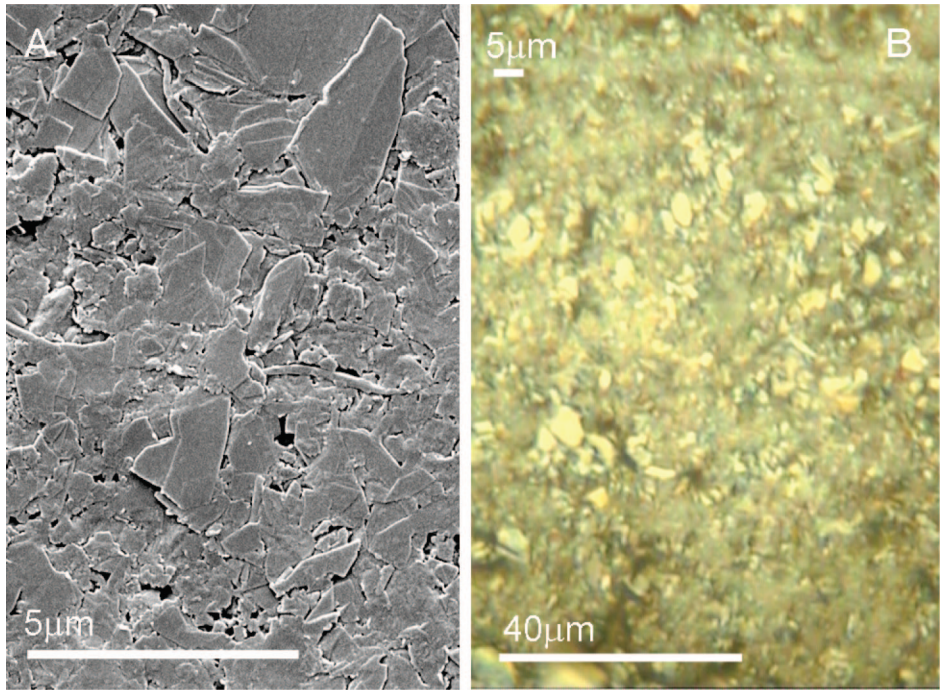

Figure 7. (A) SEM and (B) optical images of the surface of a graphene film. This film was ~150 nm thick and had been deposited on a cellulose membrane by filtration from an SDBS-based dispersion (C_{SDBS} = 0.5 mg/mL, C_G = 0.003 mg/mL). This film was not rinsed and was dried under vacuum at room temperature.

A)/ρ, where ρ is the film density. While this is not known, we estimate it as ~2000 kg/m^3, as these films are not expected to display significant porosity by analogy with graphene oxide films.[34]

2.5.1. Microscopy. Figure 7 shows SEM and optical images of a typical film (the segment of the film used for SEM was coated with 10−20 nm of gold/palladium). It can be seen from the SEM image that many of the flakes are small with diameters ~1 μm. In addition, there are some large flakes ~5 μm in diameter, which we associate with the flake shown in Figure 3E. In contrast to films cast from solvents,[14] the flakes lie flat on top of each other, suggesting the possibility of good electrical contact between flakes. The small flakes are not visible in the optical image, appearing as a uniform background. However, the large flakes are apparent, appearing as bright regions. Significant quantities of these large flakes are present.

2.5.2. Characterization of Flake Quality. It is very important to characterize the quality of the exfoliated graphene flakes. The novel electronic properties of graphene are extremely sensitive to the presence of defects such as oxides. It is critical to determine whether the exfoliation process results in the formation of defects. We do this by carrying out Raman, infrared, and X-ray photoelectron spectroscopies on thin films produced from dispersed graphene.

The deposited films were initially characterized by Raman spectroscopy. Examples of typical film spectra are given in Figure 8, alongside a spectrum for the starting graphite powder (these spectra were normalized to the intensity of the G-band at 1582 cm^{-1}). Spectra of graphitic materials are characterized by a D-band (1350 cm^{-1}), a G-band (1582 cm^{-1}), and a 2D-band (2700 cm^{-1}). The studied film had been deposited on an alumina membrane and rinsed with 17.5 mL of water before drying. As was the case in the film shown in Figure 7, this film consists of large flakes (diameter ~3−6 μm) embedded in a matrix of small flakes (diameter ~1 μm). Shown in Figure 8A are Raman spectra collected by focusing the laser spot both on the region of small flakes and on a large flake. Like the starting graphite powder, no D-band (1350 cm^{-1}) is observed in the spectrum associated with the large flake. This strongly supports the HRTEM data, showing that the dispersion process does not result in the formation of significant quantities of defects on the graphitic basal plane. In addition, the 2D-band of this large flake strongly resembles the 2D-band for graphite. This indicates that this flake is relatively thick with >5 graphene layers.[35] The relatively large diameter and thickness of such flakes allows us to associate them with the large flakes observed in Figure 3E and those that rapidly sediment out of the dispersions measured in Figure 6B. In the case of the spectrum associated with the region of small flakes, a D-band is observed. We stress that this D-band is both narrower and less intense than that reported in the literature for graphene oxide and for reduced graphene oxide.[6,9] We suggest this feature is dominated by edge effects as the Raman excitation beam spot size of ~2 μm is larger than most of the flakes in the deposited film. However, we cannot rule out the presence of a contribution from basal plane defects induced by processing. However, the relatively low D-band intensity observed for the small flakes coupled with the complete absence of a D-band for the bigger flakes strongly suggests that the films we are producing are composed of flakes with low defect content. Turning to the 2D-band associated with the small flakes, by comparison to literature,[35] its shape is characteristic of thin flakes composed of less than five graphene layers. A detailed analysis of 30 Raman spectra taken at different points on the film with the beam focused on small flakes showed every

(34) Dikin, D. A.; Stankovich, S.; Zimney, E. J.; Piner, R. D.; Dommett, G. H. B.; Evmenenko, G.; Nguyen, S. T.; Ruoff, R. S. *Nature* **2007**, *448*, 457–460.

(35) Ferrari, A. C.; Meyer, J. C.; Scardaci, V.; Casiraghi, C.; Lazzeri, M.; Mauri, F.; Piscanec, S.; Jiang, D.; Novoselov, K. S.; Roth, S.; Geim, A. K. *Phys. Rev. Lett.* **2006**, 97.

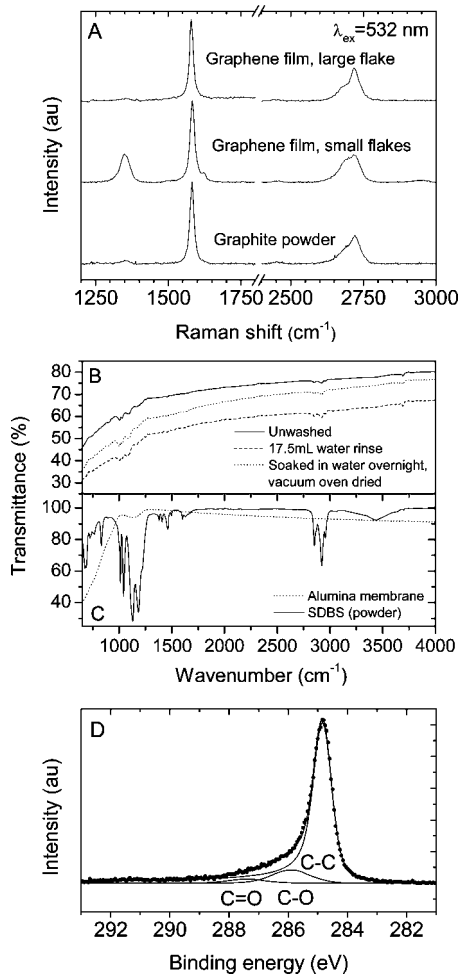

Figure 8. Characterization of flake quality. (A) Raman spectrum of a graphene film (thickness ~300 nm) deposited on an alumina membrane by filtration from an SDBS-based dispersion (C_{SDBS} = 0.5 mg/mL, C_G = 0.005 mg/mL) and rinsed with 17.5 mL of water. Spectra associated with both large flakes (diameter ~3−6 μm, top) and small flakes (diameter ~1 μm, middle) are shown. For comparison, a spectrum collected from the starting graphite powder is included (bottom). (B,C) ATR-FTIR spectra of materials used in this study. (B) Spectra of three graphene films with different washing regimes. The films were ~300 nm thick and were deposited on alumina by vacuum filtration from an SDBS-based dispersion (C_{SDBS} = 0.5 mg/mL, C_G = 0.005 mg/mL). (C) Control spectra of SDBS powder and the alumina filter membrane used to prepare the graphene films. (D) XPS spectra for a graphene thin film produced by vacuum filtration and dried in a vacuum oven at room temperature. The Shirley background has been removed. Fit lines are due to contributions from graphitic carbon (C−C), C−O, and C═O.

spectrum collected to be consistent with thin flakes consisting of <5 monolayers. This shows that while reaggregation undoubtedly occurs during filtration, the degree of reaggregation is limited.

Attenuated total reflectance (ATR) FTIR spectra of deposited films were also measured as a function of washing regime (Figure 8B), along with reference spectra for SDBS powder and the alumina membrane (Figure 8C). These spectra show only very small features at ~1100 and ~2900 cm^{-1}. By comparison with the reference spectra, it is clear that these features are attributable to residual surfactant trapped in the film. A key feature of the spectra in Figure 8B is the absence of peaks associated with C−OH (~1340 cm^{-1}) and −COOH (~1710−1720 cm^{-1}) groups.[7,36−38] Our spectra are in contrast to those in the literature for films made from reduced graphene oxide[7,38] or chemically derived graphene.[12] This is further evidence that our exfoliation technique does not chemically functionalize the graphene/graphite and that our films are composed of largely defect-free material.

However, the best test for the presence of defects in the form of oxides is X-ray photoelectron spectroscopy. A carbon 1s core level spectrum measured on a very thin vacuum deposited graphene film is shown in Figure 8D. This spectrum is dominated by a feature around 285 eV, which we associate with graphitic carbon. However, graphitic carbon alone cannot explain the entire spectrum. Fitting procedures show that two small additional lines at 286 and 287.5 eV are required, in addition to the C−C line, to fully explain the spectrum. We associate these lines with C−O and C═O groups, respectively. This shows that, in contrast to the FTIR results, low levels of oxidation of the graphite have occurred during the exfoliation/dispersion process. However, we emphasize that the levels of oxidation are small. The main C−C peak makes up 86% of the spectrum. This is similar to what is obtained when graphene oxide is thermally annealed at 1100 °C in vacuum.[10] Taken together with the Raman and FTIR results, we can conclude that while small amounts of oxidation do occur during processing, the resultant structural damage as measured by Raman spectroscopy is low. Thus, we expect the quality of the produced flakes to be high, especially when compared to graphene oxide.

Incidentally, XPS measurements show no evidence of any sulfur present in these very thin graphene films (or at least in the top few nanometers). This suggests the absence of surfactant. This is in contrast to thicker films, which contained ~35% surfactant. It is likely that the surfactant gets washed through the thin films during filtration in a manner that is impossible for the thicker films.

2.5.3. Optical and Electrical Properties. To test the optical and electrical properties of these films, we measured the transparency (632 nm) and sheet resistance of a number of vacuum deposited films (nominal thickness ~30 nm). As-deposited films typically had transmittance of ~62% coupled with sheet resistance of ~970 kΩ/□. This corresponds to a DC conductivity of 35 S/m. The low value is probably attributable to the presence of residual surfactant. As discussed above, up to 36 wt % of thick filtered films is residual surfactant, which can be difficult to remove by washing. We attempted to remove any residual surfactant by annealing @ 250 °C in Ar/N_2 for 2 h prior to remeasuring the transmittance and sheet resistance. After annealing, the transparency was unchanged while the sheet resistance had fallen to 22.5 kΩ/□, consistent with a nominal DC conductivity of 1500 S/m. This value is significantly lower than that recently measured for similar films prepared from *N*-methyl-pyrrolidone-based dispersions[14] (~6500 S/m). In addition, films of reduced graphene oxide have displayed conductivities ranging from 7200 S/m[7] to 10 000 S/m.[10] In comparison, graphene dispersed in dimethyl-acetamide has been spray-cast into films with conductivities as high as 10^5 S/m.[13] Thus, the presence of residual surfactant may impede the electrical properties of our films. However, we believe that the combination of aqueous environment and lack of defects gives our dispersion/exfoliation method great potential. Complete

(36) Hontorialucas, C.; Lopezpeinado, A. J.; Lopezgonzalez, J. D. D.; Rojascervantes, M. L.; Martinaranda, R. M. *Carbon* **1995**, *33*, 1585–1592.
(37) Titelman, G. I.; Gelman, V.; Bron, S.; Khalfin, R. L.; Cohen, Y.; Bianco-Peled, H. *Carbon* **2005**, *43*, 641–649.
(38) Si, Y.; Samulski, E. T. *Nano Lett.* **2008**, *8*, 1679–1682.

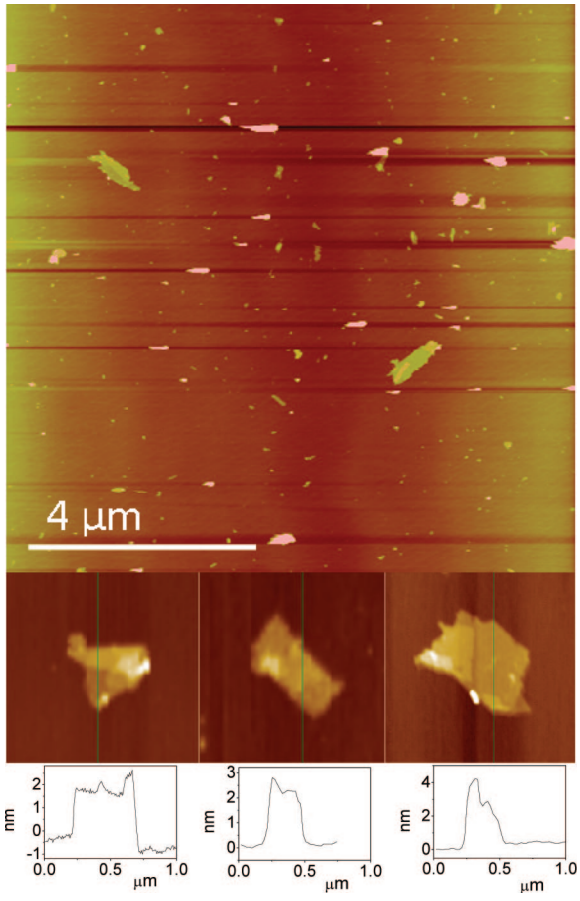

Figure 9. AFM images of spray deposited graphene. The top image shows a typical 10 μm × 10 μm square showing large numbers of graphene flakes. In the middle are three zoomed-in images of individual flakes. Below each image is a line scan taken vertically through the center of the image.

removal of surfactant may result in a material, which can challenge nanotubes as an indium tin oxide replacement material. Future work will focus on removal of residual surfactant from films, the maximization of electrical conductivity, and the deposition of films consisting predominately of individual monolayers.

2.6. Deposition of Graphene Flakes on Surfaces. Once graphene can be dispersed and exfoliated, the ability to deposit individual flakes onto surfaces is very important for further characterization. This is problematic for graphene exfoliated in amide solvents[14] as their high boiling point results in slow evaporation, allowing extensive reaggregation. We have developed a method to spray surfactant-stabilized graphene flakes onto mica (see Experimental Procedure). This is followed by surfactant removal by washing. Shown in Figure 9 is an atomic force microscopy (AFM) image of a 10 μm × 10 μm mica surface after graphene deposition. Large numbers of flakes can be seen. In addition, we observed small numbers of aggregates, characterized by heights in excess of 12 nm. While the largest flakes are similar in lateral size to those observed by TEM, many smaller, submicrometer-sized flakes can be seen. Shown in the middle part of Figure 9 are zoomed images of three of these flakes. Below each is shown a line scan illustrating its size. We measured the dimensions (height, width, and length) of a large number (182) of these flakes (ignoring the aggregates with height >12 nm). To account for tip effects, we subtract 50 nm from both width and length data. These data are presented in Figure 10 as (A) height, (B) width, and (C) length distributions.

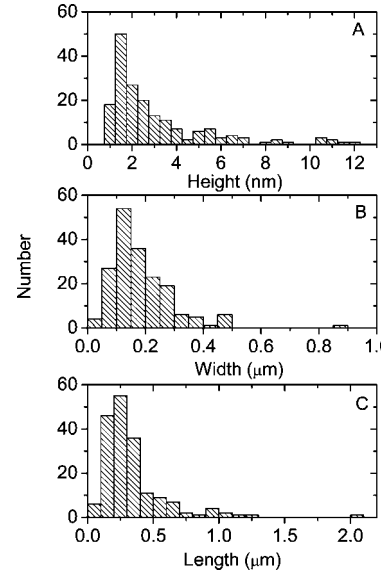

Figure 10. Statistics derived from analysis of the AFM images of 182 flakes: (A) height, (B) width, and (C) length of deposited flakes.

Most interesting are the height data, which show a peak around 1.5 nm. Many publications show the apparent height of graphene monolayers as measured by AFM to be ~1 nm. This suggests the peak represents flakes with 1−2 layers, in reasonable agreement with the TEM data shown in Figure 4. In addition, ~10% of the flakes have thickness ~1 nm, consistent with monolayer graphene.

However, the data for width and length are significantly different from the TEM data. The majority of thin flakes observed by TEM are ~1 μm wide. However, the peak widths and lengths observed by AFM are ~150 and ~250 nm, respectively. The reason for this discrepancy is unclear at present. One possibility is that during TEM sample preparation, the smaller flakes get washed through the grid, thus giving biased lateral size measurements.

As mentioned above, we also observe some graphite aggregates with heights >12 nm and lateral dimensions ranging from 300 nm to 2 μm. As some of these objects have relatively small lateral dimensions, we cannot solely link them to the large flakes that inadvertently remain in the dispersion after decantation, as observed by TEM. We believe these larger objects are exfoliated graphene flakes that have subsequently reaggregated as a result of our deposition process. Spraying the dispersion onto heated mica yields significant quantities of exfoliated graphene but also an extensive coating of SDBS. We find it necessary to wash the substrate with water to remove this residual SDBS. We speculate that this washing not only removes SDBS from the mica but also from the deposited graphene. In addition, it is likely that the deposited graphene is at least partially mobile during the washing phase. Any mobile, uncoated graphene sheets will be unstable against reaggregation. It is likely that during the washing/drying of the substrate some of these newly formed aggregates are left behind on the mica surface in addition to the exfoliated material. This is supported by the fact that the population of aggregates depends critically on the details of the washing/drying process. Further work is underway to improve this deposition/washing procedure. However, despite the presence of the aggregates, we can still easily observe thin exfoliated graphene material as shown in Figure 10.

3. Conclusion

We have developed a method to disperse graphite in surfactant−water solutions with the aid of ultrasound. This results in large-scale exfoliation to give large quantities of multilayer graphene with <5 layers and smaller quantities of monolayer graphene. The exfoliated flakes are stabilized against reaggregation by a relatively large potential barrier, which originates in the Coulomb repulsion between surfactant-coated sheets. The dispersions are reasonably stable with larger flakes sedimenting out over ~6 weeks. These dispersions can be used to form films by vacuum filtration or to deposit individual flakes by spray coating. Characterization of the films by HRTEM, Raman, IR, and X-ray photoelectron spectroscopy suggests only low levels of defects or oxides on the graphene basal plane. These films are reasonably conductive and can be made semitransparent. It is anticipated that their properties can be significantly enhanced by improved surfactant removal.

4. Experimental Procedure

The graphite powder used in all experiments was purchased from Sigma Aldrich (product number 332461) and sieved through a 0.5 mm mesh to remove large particles. Sodium dodecylbenzene sulfonate (SDBS) was purchased from Sigma Aldrich (lot no. 065K2511) and used as provided. Stock solutions of SDBS of concentrations between 5 and 10 mg/mL were prepared in Millipore water by stirring overnight. A typical sample was prepared by dispersing graphite in the desired SDBS concentration (25 mL sample volume in cylindrical vials) using 30 min of sonication in a low power sonic bath (Branson 1510E-MT bath sonicator). The resulting dispersion was left to stand for approximately 24 h to allow any unstable aggregates to form and then centrifuged for 90 min at 500 rpm (Hettich Mikro 22R). After centrifugation (CF), the top 15 mL of the dispersion was decanted by pipet and retained for use. For optical characterization, a range of graphene concentrations were prepared. To maintain the surfactant concentration after dilution, all dilutions were carried out by adding surfactant solution with C_{SDBS} identical to the graphene dispersion being diluted.

Absorption measurements were taken using a Varian Cary 6000i with quartz cuvettes. Sedimentation profiles were taken with a homemade apparatus using an array of synchronized pulsed lasers and photodiodes.[31] TEM samples were prepared by pipetting a few milliliters of this dispersion onto holey carbon mesh grids (400 mesh). Bright-field TEM images were taken with a Jeol 2100, operated at 200 kV. HRTEM images were taken with the Oxford-JEOL JEM2200MCO FEGTEM/STEM, fitted with two CEOS Cs aberration correctors, operated at 200 kV.

Zeta potential measurements were carried out on a Malvern Zetasizer Nano system with irradiation from a 633 nm He−Ne laser. The samples were injected in folded capillary cells, and the electrophoretic mobility (μ) was measured using a combination of electrophoresis and laser Doppler velocimetry techniques. The electrophoretic mobility relates the drift velocity of a colloid (v) to the applied electric field (E), $v = \mu E$. All measurements were conducted at 20 °C and at the natural pH of the surfactant solution unless otherwise stated. The ζ-potential can be calculated (in SI units) from the electrophoretic mobility using the Smoluchowski expression for plate-like particles:[28] $\zeta = \eta\mu/\varepsilon$, where η is the solution viscosity, and ε is the solution permittivity, $\varepsilon = \varepsilon_r\varepsilon_0$. This expression applies for plates with uniform surface charge, which are large enough for edge charge to be neglected and whose radius is much larger than the double layer thickness.[39] As the double layer thickness is ~8.1 nm in our samples, we believe that these criteria hold here.

Samples for AFM were prepared by spray-casting the dispersion onto freshly cleaved mica. 1 mL of the dispersion was sprayed over the mica using an Evolution Airbrush (www.graphics.co.uk) spray gun. The mica surface was maintained at 120 °C using a hotplate. The gun was held approximately 20 cm from the mica surface and set to deliver a fine mist of the dispersion using a pressure of 1.5 bar. This method allowed the water to flash evaporate from the surface of the mica. After approximately 0.5 mL of dispersion had been dispensed, the sample was rinsed by immersion in a water bath for 30 s and gently dried with compressed air. The remaining 0.5 mL of dispersion was sprayed on, and the sample was rinsed again. AFM measurements were taken with a Digital Instruments Nanoscope IIIA from Veeco Systems in tapping mode using silicon tips with a resonance frequency of 320 kHz.

Preparation of a typical film was carried out immediately after CF by vacuum filtration of the dispersion through nitrocellulose membranes (pore size 25 nm) or alumina membranes (pore size 20 nm) supported on a fritted glass holder. In some cases, the resulting compact films were washed with water and dried overnight in a vacuum oven at room temperature at 10^{-3} mbar. The film thickness, t, could be estimated from the known deposited mass per unit area, M/A, using $t = (M/A)/\rho$, where ρ is the film density. While this is not known, we estimate it as ~2000 kg/m^3, as these films are not expected to display significant porosity by analogy with graphene oxide films.[34] SEM analysis was carried out in a Hitachi S-4300 field emission SEM. Raman spectra were taken on a Horiba Jobin Yvon LabRAM-HR using a 100× objective lens with a 532 nm laser excitation. Attenuated total reflectance FTIR spectra of these films were taken on a Perkin-Elmer Spectrum 100. X-ray photoelectron spectroscopy (XPS) was performed in a system equipped with a VG CLAM II electron analyzer and PSP twin anode source. Mg Kα ($h\nu$ = 1253.6 eV) spectra were recorded at 10 eV pass energy and 2 mm slits, yielding an overall energy resolution of 0.85 eV. Samples were introduced via a loadlock, and measurement base pressure was better than 10^{-9} mbar.

Thermogravimetric analysis was carried out on a thick film using a Perkin-Elmer Pyris 1 TGA in an oxygen atmosphere. The temperature was scanned from 25 to 900 at 10 °C/min. The optical transparency of deposited thin films, when required, was determined by comparing the transmitted intensity of a HeNe laser (632 nm) through the film to the transmitted intensity through the filter membrane alone. Annealing of some of these deposited films (on alumina membranes) was carried out in a GERO Hochtemperaturöfen GmbH tube furnace. Electrical measurements to determine the sheet resistance of the films were made using the four-probe technique with silver paint as electrodes and a Keithley 2400 source meter.

Acknowledgment. We would like to acknowledge IRCSET and Science Foundation Ireland, through the Principal Investigator scheme, for financial support.

Supporting Information Available: A derivation of the van der Waals potential energy of attraction for two parallel, two-dimensional sheets, and the full citation for ref 14. This material is available free of charge via the Internet at http://pubs.acs.org.

JA807449U

(39) Sherwood, J. D.; Stone, H. A. *Phys. Fluids* **1995**, *7*, 697–705.